Strongly Deformed TCNQ Derivatives: Syntheses and Properties of 7,12-Bis(dicyanomethylene)-7,12-dihydrobenz[*a*]-anthracene (BDCNBA) Derivatives

Kazuhiro MARUYAMA,* Hiroshi IMAHORI, Katsuhiko NAKAGAWA,† and Nobuo TANAKA††
Department of Chemistry, Faculy of Science, Kyoto University, Kyoto 606
†Department of Industrial Chemistry, Niihama National College of Technology, Niihama 792
††Department of Life Science, Faculty of Science, Tokyo Institute of Technology, Yokohama 227
(Received November 26, 1988)

In spite of large steric repulsion between aromatic quinone moiety and dicyanomethylene moiety the title compounds (BDCNBA) were synthesized by $TiCl_4$-catalyzed reactions of the corresponding aromatic quinones and malononitrile. BDCNBA showed electronic spectra indicating the intramolecular charge-transfer interaction and redox properties similar to 11,11,12,12-tetracyano-9,10-anthraquinodimethane (TCNAQ) derivatives. BDCNBA showed a low electrical conductivity ($\approx 10^{-7}\ \Omega^{-1}\ cm^{-1}$). Strongly deformed structure of BDCNBA was established by X-ray crystallographic analysis.

Recently much attentions have been centered to organic metals.[1] Organic metals are generally composed of donors and acceptors, but acceptors investigated so far have been limited mostly to tetracyanoquinodimethane (TCNQ) analogues, while a variety of donors have been examined. 11,11,12,12-Tetracyano-9,10-anthraquinodimethane (TCNAQ) deviates deform from flat molecular plane of the corresponding anthraquinone, having butterfly form, because of steric repulsion between peri-hydrogen of aromatic moiety and dicyanomethylene group.[2] Nevertheless they make complex with aromatic donors in many cases.[3] It is important to elucidate the relationship between steric factor in organic metals and complex formation between donors and acceptors or electrical conductivity for designing excellent organic metals. We synthesized polyaromatic TCNQ compounds to investigate the effect of aromaticity and steric repulsion between dicyanomethylene moiety and aromatic moiety by introducing a benzene ring to TCNAQ framework. Now we wish to report here syntheses and properties of 7,12-bis(dicyanomethylene)-7,12-dihydrobenz[*a*]anthracene derivatives.

Table 1. $TiCl_4$-Catalyzed Reaction between Quinone **1** and Malononitrile

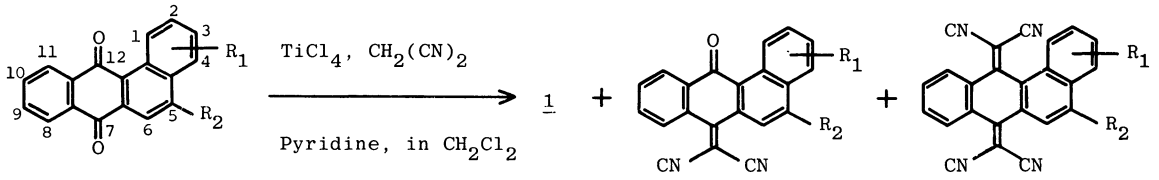

Run		Quinone **1**	Quinone conversion/%	Yields of products/% **2**		**3**	
1	**1a**:	R_1=2-F, R_2=H	100	**2a**:	0	**3a**:	70
2	**1b**:	R_1=2-Cl, R_2=H	100	**2b**:	0	**3b**:	64
3	**1c**:	R_1=2-H, R_2=H	100	**2c**:	0	**3c**:	88
4	**1d**:	R_1=2-Me, R_2=H	100	**2d**:	0	**3d**:	64
5	**1e**:	R_1=2-OMe, R_2=H	100	**2e**:	0	**3e**:	70
6	**1f**:	R_1=3-OMe, R_2=H	100	**2f**:	0	**3f**:	48
7	**1g**:	R_1=4-OMe, R_2=H	100	**2g**:	0	**3g**:	70
8	**1h**:	R_1=2-F, R_2=4-FC_6H_4	100	**2h**:	53	**3h**:	40
9	**1i**:	R_1=2-Cl, R_2=4-ClC_6H_4	63	**2i**:	8	**3i**:	22
10	**1j**:	R_1=2-H, R_2=C_6H_5	100	**2j**:	80	**3j**:	18
11	**1k**:	R_1=2-Me, R_2=4-MeC_6H_4	96	**2k**:	74	**3k**:	21
12	**1l**:	R_1=2-OMe, R_2=4-$OMeC_6H_4$	97	**2l**:	63	**3l**:	30
13	**4**:	5,12-naphthacenequinone	100	**5**:	0	**6**:	60

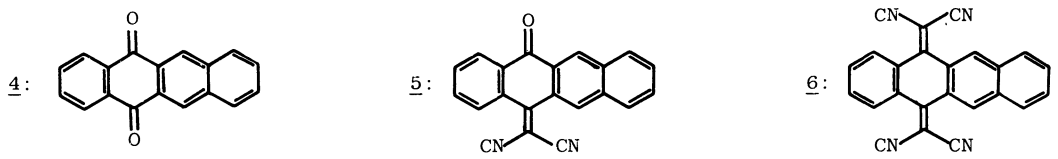

Results and Discussion

Synthesis of BDCNBA. 7,12-Bis(dicyanomethylene)-7,12-dihydrobenz[*a*]anthracenes (BDCNBA) **3** were synthesized from the corresponding benz[*a*]anthracene-7,12-diones **1** according to the Aumüller[4] and Ong[5] method. The results are summarized in Table 1. In spite of large steric repulsion between dicyanomethylene groups and aromatic moieties, especially naphthalene moiety, BDCNBA **3a—g** were produced in high yields compared to the case of TCNAQ,[3-6] while 7-(dicyanomethylene)benz[*a*]anthracen-12(7*H*)-ones (DCNBA) **2a—g** were not obtained. 5,12-Bis-(dicyanomethylene)-5,12-dihydronaphthacene **6** which is less crowded than **3c** was also obtained in similar yield. In Runs 8—12, BDCNBA **3h—l** were obtained in low yields, whereas DCNBA **2h—l** were obtained majorly. The respective structures of compounds **2**, **3** were assigned by the spectroscopic data as well as X-ray analyses of **2j** and **3c**. A proton at C-1 of **2** showed characteristic shift in the ^{1}H NMR spectrum ($\delta \approx 9$—10) similar to that in the corresponding quinone **1** due to the additional deshielding of carbonyl group, while no similar downfield shift of C-1 proton in the ^{1}H NMR spectrum of the corresponding BDCNBA **3** was observed (see Experimental section). This indicates that the position of dicyanomethylene group in **2** probably is at less crowded C-7 site. The structure was unambiguously determined by X-ray analysis of **2j**. It is known that only 1,3-dimethyl-10-(dicyanomethylene)anthrone was formed exclusively when 1,3-dimethylanthraquinone was subjected to the same reaction,[5] while 1,5-dichloro-9,10-bis(dicyanomethylene)-9,10-dihydroanthracene was obtained in a low yield (19%) when the corresponding anthraquinone was used.[4] In our case it is amazing that BDCNBA **3** was produced in a high yield in spite of supposedly larger steric repulsion between aromatic moieties and dicyanomethylene groups compared to other cases.

UV-Visible Absorption Spectrum. The UV-visible absorption spectrum of BDCNBA **3c** in dichloromethane shows bands at 231 ($\log \varepsilon$=4.29), 285 (4.19), 337 (4.46), and 431 (3.46) nm. Thus, the lowest energy electronic transition (λ_{max}=431 nm) is red-shifted by ca. 80, 30, 30 nm, compared to those of TCNAQ,[7] 9,9,10,10-tetracyano-1,4-naphthoquinodimethane (TCNNQ),[7] tetracyanoquinodimethane (TCNQ), respectively (Table 2). In addition, the longest wavelength band (λ_{max}) of TCNAQ is blue-shifted by ca. 70 nm compared with that of anthraquinone, while that of **3c** is red-shifted by ca. 100 nm compared with that of **1c** (Table 2). It is well-known that the central ring in TCNAQ is bent into a boat form and the two benzene rings are noncoplanar to avoid the severe steric interactions between the cyano groups and the peri-hydrogens.[2] Since the structure of **3c** deforms more severely than that of TCNAQ as discussed later, the observed large red shift (λ_{max}) in the longest wavelength band is unusual. These data suggest that the large red shift of the longest wavelength bands is not ascribed to the larger delocalization of the π system, but to the intramolecular charge-transfer (CT) interaction[8] between dicyanomethylene groups and aromatic moieties. The peak values (λ_{max}^{CT}) in the longest wavelength region were more blue-shifted for **3a—g** and **3h—l**, as electron-withdrawing substituent groups were introduced into the naphthalene moiety (Table 3). As the polarity of solvent increased,[9] blue shifts of the λ_{max}^{CT} were observed in the UV spectra of **3c** and **3j** (Table 4). Since the corresponding CT band

Table 3. Longest Wavelength Band (λ_{max}^{CT}) of **2** and **3** in CH_2Cl_2

3	λ_{max}^{CT}/nm	**3**	λ_{max}^{CT}/nm	**2**	λ_{max}^{CT}/nm
3a	424	**3h**	449	**2h**	422
3b	426	**3i**	458	**2i**	425
3c	431	**3j**	458	**2j**	427
3d	444	**3k**	478	**2k**	450
3e	474	**3l**	502	**2l**	477
3f	462				
3g	480				
6	424				

Table 4. Solvent Effects for CT Band

Solvent	*Z* value[a]	λ_{max}^{CT}/nm[b] **3c**	**3j**	**2j**
C_6H_6	54	433	459	432
CH_2Cl_2	64.2	431	458	427
CH_3CN	71.3	418	441	420
CH_3OH	83.6	416	438	—[c]

a) Kosower's solvent parameter.[9] b) Measured at 1.0×10^{-4} mol dm^{-3}. c) For low solubility of **2j** in methanol.

Table 2. UV-Visible Spectra of TCNQ Derivatives in CH_2Cl_2

Compound	λ_{max} ($\log \varepsilon$)/nm
TCNQ	235 (3.57), 380 (4.42), 401 (4.63)
TCNNQ	290 (3.89), 388 (4.53), 404 (4.50)[a]
9,10-Anthraquinone	253 (4.73), 264 (4.33), 274 (4.26), 326 (3.76), 414 (1.90)
TCNAQ	283 (4.48), 305 (4.22), 347 (4.43)[a]
1c	242 (4.41), 249 (4.35), 284 (4.55), 336 (3.65)
3c	231 (4.29), 285 (4.19), 337 (4.46), 431 (3.46)

a) From Ref. 7.

was also observed in **6**, these effects are not due to the deformation derived from larger steric interaction compared to TCNAQ, but due to the easier electron-releasing character from naphthalene moiety to dicyanomethylene group caused by replacement of benzene ring to naphthalene one. Indeed, similar substituent (Table 3) and solvent effects (Table 4) in **2h—l** were observed. That is, the values of λ_{max}^{CT} were blue-shifted as electron-withdrawing substituent groups were introduced in the naphthalene moiety. The similar inclination was observed as the polarity of solvent increased. Thus, these longest bands are due to the intramolecular CT interaction.

Electrochemical Studies. Table 5 shows the results of cyclic voltammogram of TCNQ derivatives in acetonitrile, taken at room temperature using with tetraethylammonium perchlorate as the supporting electrolyte. For BDCNBA only one reversible redox wave, which corresponds to two electron reduction observed in the case of TCNAQ,[2-4,7] was observed in the range from 0 to −2.0 V and the value of $E_{1/2}^{red}$ is much lower than that in TCNQ, but is a little lower than that in TCNAQ. These facts suggest that extension of aromatic system contributes only slightly to the reduction potential, but decrease of the aromaticity due to big steric repulsion between dicyanomethylene groups and aromatic moieties has a greater effect. From the value of $E_{1/2}^{red}(1)-E_{1/2}^{red}(2)$ (+0.016) obtained by Myers and Shain's method,[10] we can estimate the value of semiquinone formation constant K_{sem} as the following;

$$\log K_{sem} = \log([BDCNBA^{-}]^2/[BDCNBA][BDCNBA^{2-}]) = (E_{1/2}^{red}(1) - E_{1/2}^{red}(2))/0.058$$

The small log K_{sem} (+0.28) value of **3c** relative to that of TCNQ, but nearly equal to that of TCNAQ indicates that anion radical **3c**$^{-}$ is unstable. It has been concluded from the ESR and the ENDOR studies of TCNQ derivatives that the negative charges in the dianions tend to localize on the two dicyanomethylene groups.[11] This inclination is enhanced in TCNAQ^{2-} because of the steric repulsion between peri-hydrogen and dicyanomethylene group.[6,7] Since C7—C13 and C12—C16 bonds (see Fig. 2) turn to be single in the dianion of **3c**, steric repulsion between dicyanomethylene groups and aromatic moieties including peri-hydrogen atoms in **3c**$^{2-}$ would be readily released by twisting the two negatively charged dicyanomethylene groups out of the aromatic plane rather than by bending the central benzene ring (consisting of C6a, C7, C7a, C11a, C12, C12a) in the benz[*a*]anthracene moiety. Thus, disproportionation between dianion **3c**$^{2-}$ and **3c** easily would occur because of the steric interaction.[12]

Table 5. Reduction Potentials[a] and Semiquinone Formation Constants of TCNQ Derivatives

Compound	$E_{1/2}^{red}$ (1)	$E_{1/2}^{red}$ (2)	log K_{sem}[e]
TCNQ[b]	+0.18	−0.36	9.31
TCNAQ[c]	−0.37		−0.03
BDCNBA[d]	−0.44		+0.28

a) V vs. SCE, 0.1 mol dm^{-3} Et_4NClO_4 in CH_3CN, platinum electrode. b) From Ref. 6. c) From Ref. 3. d) This work. e) From Ref. 10.

Electrical Conductivity. Mukai et al. reported that TCNAQ forms CT complex with many aromatic donors and steric factor is important to form complexation.[3,6] On the contrary, 2,3,5,6-tetramethyl-7,7,8,8-tetracyanoquinodimethane (TMTCNQ), which has strong deformation of the TCNQ skeleton into a boat-conformation,[13] formed no complex with tetrathiafulvalene (TTF), tetramethyltetrathiafulvalene (TMTTF), tetramethyltetraselenafulvalene (TMTSF).[14] In our case, no complex was formed between **3c** and a variety of electron donors, like as naphthalene, pyrene, anthracene, TMTTF, although they showed charge-transfer bands in dichloromethane solution similar to the cases observed between TCNAQ and aromatic donors (Table 6 and Experimental section), indicating that the larger steric hindrance between donor and

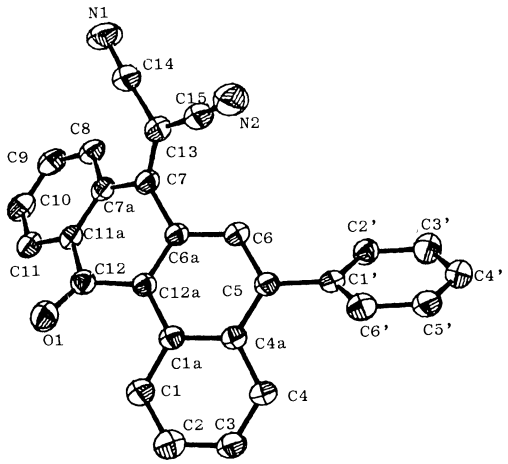

Fig. 1. ORTEP view of **2j**.

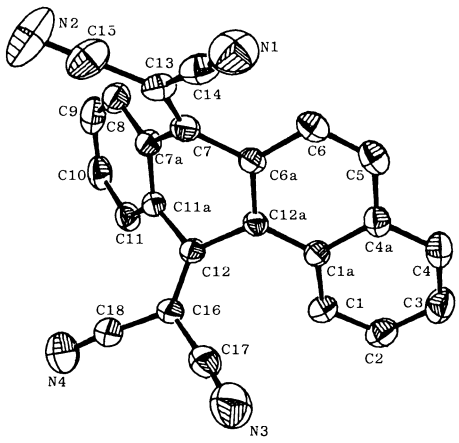

Fig. 2. ORTEP view of **3c**.

acceptor interrupts the complex formation.

It is well-known that partial charge transfer from donor to acceptor is important for high quality of organic metals.[1] Thus, **3c** itself has possibility of showing high electrical conductivity, since **3c** has intramolecular CT character. Against our expectation, **3c** showed low electrical conductivity (1×10^{-7} Ω^{-1} cm^{-1}) at room temperature. These results suggest that large steric deformation reduces intermolecular interaction and results in low electrical conductivity.

X-Ray Structures of DCNBA 2j and BDCNBA 3c. The structures of DCNBA and BDCNBA frameworks were definitely confirmed by X-ray diffraction analyses of **2j** and **3c** (Figs. 1 and 2). The atomic positional and equivalent isotropic thermal parameters are listed in Table 7. Bond distances and angles of **2j** and **3c** are listed in Tables 8 and 9, respectively.

Table 6. Charge-Transfer Absorption Maxima of BDCNBA **3c** and Aromatic Donors[a] (λ_{max}/nm in CH_2Cl_2)

Naphthalene	Pyrene	Anthracene	TMTTF
485	502	518	632

a) BDCNBA: 2.5×10^{-3} mol dm^{-3}, donors: 5.0×10^{-2} mol dm^{-3}.

Bond lengths and angles of TCNQ unit (consisting of C6a, C7, C7a, C11a, C12, C12a) in **3c** are almost the same as those in TCNAQ. However, deformation of the structure of **3c** is larger than that of TCNAQ. The dihedral angle between planes A (consisting of C8, C9, C10, C11, C11a, C7a) and B (consisting of C1, C2, C3, C4, C4a, C5, C6, C6a, C12a, C1a) is 49.5° for **3c**, while that of TCNAQ is 35.4° (see Fig. 2 and Table 10). The dihedral angle between planes A and B in **2j** is 33.3°, and that in 10-dicyanomethyleneanthrone is 28°.[15] These facts indicate that introduction of naphthalene unit into TCNAQ causes the larger deformation of the structure because of the steric repulsion between naphthalene moiety and dicyanomethylene group. Comparison of bond distances of naphthalene moiety for benz[a]anthracene-7,12-dione vs. **3c** or **2j** reveals us degree of the deformation for naphthalene moiety, for example, 142.0 pm for **3c**, 144.4 pm for **2j** vs. 147.2 pm for 8-methylbenz[a]anthracene-7,12-dione (MBAD) (C1a–C12a); 134.8 pm for **3c**, 138.5 pm for **2j** vs. 139.3 pm for MBAD (C5–C6).[16] Thus, bond lengths of naphthalene moiety in **3c** and **2j** (C1–C1a, C1a–C12a, C6a–C12a, C6–C6a, C5–C6, C4a–C5, C4–C4a) are different from those in MBAD due to effect of the butterfly form. On the other hand, bond lengths of

Table 7. Atomic Positional and Equivalent Isotropic Thermal Parameters for **2j** and **3c**

2j					**3c**				
Atom	x	y	z	B_{eq}/B_{iso}[a]	Atom	x	y	z	B_{eq}/B_{iso}[a]
O1	0.3136(2)	0.6576(2)	0.1908(3)	4.2	N1	0.6169(4)	0.7284(2)	0.8259(5)	5.1
N1	−0.1948(3)	0.7725(3)	0.0408(5)	5.4	N2	0.7082(5)	0.9748(3)	0.5380(5)	7.3
N2	0.0910(3)	1.1228(3)	0.3780(5)	5.4	N3	−0.2323(4)	0.7063(2)	0.4057(5)	4.9
C1	0.5652(3)	0.8909(3)	0.2914(4)	3.2	N4	−0.1311(4)	0.9332(2)	0.0911(6)	5.9
C2	0.6957(3)	0.9657(3)	0.3538(4)	3.7	C1	−0.1759(4)	0.5558(2)	0.1029(4)	3.0
C3	0.7596(3)	1.1056(3)	0.3796(4)	3.6	C2	−0.2764(4)	0.4676(2)	0.0778(5)	3.6
C4	0.6909(3)	1.1692(3)	0.3473(4)	3.3	C3	−0.2137(4)	0.3937(2)	0.1634(5)	3.8
C5	0.4811(3)	1.1635(3)	0.2566(4)	2.8	C4	−0.0489(4)	0.4090(2)	0.2680(5)	3.4
C6	0.3503(3)	1.0867(3)	0.1888(4)	3.0	C5	0.2334(4)	0.5143(2)	0.3984(5)	3.1
C7	0.1457(3)	0.8653(3)	0.0800(4)	3.0	C6	0.3400(4)	0.5986(2)	0.4194(4)	3.0
C8	0.0046(3)	0.6681(3)	−0.1817(4)	3.5	C7	0.3916(3)	0.7673(2)	0.3497(4)	2.6
C9	−0.0277(3)	0.5384(4)	−0.2867(4)	4.0	C8	0.4494(4)	0.8588(2)	0.0827(5)	3.3
C10	0.0381(3)	0.4697(3)	−0.2559(4)	3.9	C9	0.3868(4)	0.8914(2)	−0.0983(5)	3.7
C11	0.1379(3)	0.5298(3)	−0.1187(4)	3.5	C10	0.2179(5)	0.8812(2)	−0.1898(5)	3.8
C12	0.2835(3)	0.7271(3)	0.1284(4)	3.0	C11	0.1083(4)	0.8374(2)	−0.1019(5)	3.2
C13	0.0556(3)	0.9085(3)	0.1360(4)	3.4	C12	0.0614(3)	0.7492(2)	0.1736(4)	2.4
C14	−0.0835(3)	0.8290(3)	0.0790(4)	3.8	C13	0.5278(4)	0.8079(2)	0.5103(5)	3.2
C15	0.0829(3)	1.0307(3)	0.2716(5)	3.9	C14	0.5767(4)	0.7623(2)	0.6858(5)	3.6
C1a	0.4904(3)	0.9531(3)	0.2550(4)	2.7	C15	0.6290(4)	0.9010(3)	0.5222(5)	4.4
C4a	0.5540(3)	1.0968(3)	0.2884(4)	2.7	C16	−0.0576(3)	0.7812(2)	0.2040(4)	2.7
C6a	0.2869(3)	0.9451(3)	0.1508(4)	2.8	C17	−0.1548(4)	0.7364(2)	0.3156(5)	3.3
C7a	0.1058(3)	0.7301(3)	−0.0439(4)	3.0	C18	−0.0936(4)	0.8672(2)	0.1394(5)	3.5
C11a	0.1733(3)	0.6607(3)	−0.0148(4)	2.9	C1a	−0.0037(3)	0.5750(2)	0.2179(4)	2.4
C12a	0.3546(3)	0.8773(3)	0.1809(4)	2.7	C4a	0.0606(4)	0.4988(2)	0.2979(4)	2.8
C1′	0.5416(3)	1.3125(3)	0.2955(4)	2.8	C6a	0.2800(3)	0.6754(2)	0.3430(4)	2.5
C2′	0.6128(3)	1.3988(3)	0.4569(4)	3.2	C7a	0.3403(4)	0.8129(2)	0.1692(4)	2.6
C3′	0.6686(3)	1.5384(3)	0.4932(4)	3.6	C11a	0.1683(3)	0.8021(2)	0.0754(4)	2.5
C4′	0.6532(3)	1.5936(3)	0.3680(5)	4.1	C12a	0.1097(3)	0.6641(2)	0.2486(4)	2.3
C5′	0.5809(3)	1.5094(3)	0.2076(5)	4.3					
C6′	0.5238(3)	1.3683(3)	0.1723(4)	3.3					

a) $B_{eq}=\frac{4}{3}(B_{11}a^2+B_{22}b^2+B_{33}c^2+B_{12}ab\cos\gamma+B_{13}ac\cos\beta+B_{23}bc\cos\alpha))$.

Table 8. Bond Distances for **2j** and **3c**

From To	Distance/pm	ESD	From To	Distance/pm	ESD
		2j			
O1–C12	122.9	0.4	N1–C14	114.8	0.5
N2–C15	114.0	0.5	C1–C2	137.1	0.5
C1–C1a	142.5	0.5	C2–C3	140.8	0.5
C3–C4	136.8	0.5	C4–C4a	142.7	0.5
C5–C6	138.5	0.5	C5–C4a	143.7	0.5
C5–C1′	148.9	0.5	C6–C6a	141.3	0.5
C7–C13	136.2	0.5	C7–C6a	148.9	0.5
C7–C7a	147.7	0.5	C8–C9	139.0	0.6
C8–C7a	140.4	0.5	C9–C10	138.9	0.6
C10–C11	139.2	0.5	C11–C11a	139.2	0.5
C12–C11a	149.3	0.5	C12–C12a	149.3	0.5
C13–C14	144.8	0.5	C13–C15	143.9	0.5
C1a–C4a	143.8	0.5	C1a–C12a	144.4	0.5
C6a–C12a	139.4	0.5	C7a–C11a	140.6	0.5
C1′–C2′	140.2	0.5	C1′–C6′	140.2	0.5
C2′–C3′	139.5	0.5	C3′–C4′	140.0	0.5
C4′–C5′	139.4	0.6	C5′–C6′	141.1	0.5
		3c			
N1–C14	113.3	0.5	N2–C15	113.3	0.6
N3–C17	113.6	0.5	N4–C18	113.4	0.6
C1–C2	136.8	0.5	C1–C1a	142.4	0.5
C2–C3	140.9	0.5	C3–C4	136.0	0.6
C4–C4a	141.5	0.5	C5–C6	134.8	0.5
C5–C4a	141.5	0.5	C6–C6a	141.9	0.4
C7–C13	136.4	0.5	C7–C6a	147.3	0.4
C7–C7a	147.5	0.4	C8–C9	139.3	0.5
C8–C7a	139.0	0.5	C9–C10	138.8	0.6
C10–C11	139.1	0.5	C11–C11a	138.7	0.5
C12–C16	134.4	0.4	C12–C11a	147.5	0.4
C12–C12a	148.8	0.4	C13–C14	144.3	0.5
C13–C15	144.3	0.5	C16–C17	144.7	0.5
C16–C18	144.1	0.5	C1a–C4a	143.5	0.5
C1a–C12a	142.0	0.4	C6a–C12a	139.8	0.4
C7a–C11a	141.2	0.4			

C1–C2, C2–C3, and C3–C4 in **3c** and **2j** are similar to those in MBAD due to the less effect of the butterfly form. The larger values of dihedral angle between planes A and C (consisting of C6a, C7a, C11a, C12a) (25.2°) or planes B and C (24.4°) compared to that of TCNNQ (15.3°),[17] TCNAQ (16.6°, 18.9°),[2] tetracyanobianthraquinodimethane (TBAQ) (23.6°, 26.1°),[18] and **2j** (15.1°, 18.3°) show that planes A and B in **3c** are more folded out of the central ring plane C than those in TCNQ derivatives. Planes D (consisting of C6a, C7, C7a, C13) and F (consisting of C16, C12, C11a, C12a) are tilted more sharply from the central ring plane C by 34.4°, 41.0°, respectively than those of TCNNQ (16.7°, 21.6°), TCNAQ (30.1°, 30.7°), TBAQ (29.8°, 35.4°), and **2j** (33.1°). Dihedral angle between planes D and E (consisting of C7, C13, C14, C15, N1, N2) (3.6°) or planes F and G (consisting of C12, C16, C17, C18, N3, N4) (3.9°) is small, thus, planes D and E (or planes F and G) are almost coplanar. Yamaguchi et al.[18] reported that TBAQ, which is the most strongly deformed of all TCNQ derivatives, was synthesized from bianthron and malononitrile, while tetracyanodiphenoquinodimethane could not be synthesized. Comparison of the corresponding dihedral angles of TBAQ and BDCNBA **3c** reveals that BDCNBA is more strongly deformed than TBAQ.

In conclusion, BDCNBA and TCNAQ are very similar except that BDCNBA shows intramolecular CT character. BDCNBA has the most strongly deformed structure of all TCNQ derivatives due to the steric interaction between benzene rings and dicyanomethylene groups.

Experimental

General Procedures. All melting points were determined with a Yanagimoto micro melting point apparatus and uncorrected. Mass spectra were taken on a JEOL JMS-DX 300 mass spectrometer. The electronic spectra were obtained by Shimadzu UV-200 spectrometer. ^{1}H NMR spectra were taken by using a JEOL-JNM-PS-100 spectrometer or a JEOL JNM-GX-400 spectrometer and chemical shifts were recorded in parts per million (ppm) on the δ scale from tetramethylsilane as an internal standard. IR spectra were obtained by using a JASCO IRA-1 spectrometer on KBr

Table 9. Bond Angles for **2j** and **3c**

	Angle/degree	ESD		Angle/degree	ESD		Angle/degree	ESD
				2j				
C2-C1-C1a	120.89	0.33	C1-C2-C3	120.68	0.35	C2-C3-C4	120.18	0.35
C3-C4-C4a	121.36	0.33	C6-C5-C4a	118.95	0.30	C6-C5-C1′	119.03	0.30
C4a′-C5-C1′	122.02	0.29	C5-C6-C6a	121.72	0.31	C13-C7-C6a	122.39	0.31
C13-C7-C7a	121.14	0.31	C6a-C7-C7a	116.24	0.29	C9-C8-C7a	119.25	0.35
C8-C9-C10	120.84	0.37	C9-C10-C11	120.40	0.36	C10-C11-C11a	119.39	0.33
O1-C12-C11a	119.74	0.30	O1-C12-C12a	124.23	0.31	C11a-C12-C12a	115.97	0.28
C7-C13-C14	123.67	0.33	C7-C13-C15	125.07	0.33	C14-C13-C15	110.94	0.32
N1-C14-C13	175.62	0.42	N2-C15-C13	172.99	0.42	C1-C1a-C4a	118.55	0.30
C1-C1a-C12a	122.67	0.30	C4a-C1a-C12a	118.75	0.29	C4-C4a-C5	121.57	0.30
C4-C4a-C1a	118.24	0.30	C5-C4a-C1a	120.15	0.29	C6-C6a-C7	120.55	0.30
C6-C6a-C12a	120.79	0.30	C7-C6a-C12a	118.65	0.29	C7-C7a-C8	124.20	0.31
C7-C7a-C11a	116.12	0.30	C8-C7a-C11a	119.65	0.32	C11-C11a-C12	119.45	0.30
C11-C11a-C7a	120.44	0.31	C12-C11a-C7a	120.12	0.30	C12-C12a-C1a	122.54	0.29
C12-C12a-C6a	117.85	0.29	C1a-C12a-C6a	119.57	0.30	C5-C1′-C2′	120.96	0.30
C5-C1′-C6′	120.01	0.30	C2′-C1′-C6′	118.99	0.31	C1′-C2′-C3′	120.75	0.33
C2′-C3′-C4′	119.99	0.35	C3′-C4′-C5′	120.11	0.36	C4′-C5′-C6′	119.64	0.35
C1′-C6′-C5′	120.48	0.33						
				3c				
C2-C1-C1a	120.26	0.31	C1-C2-C3	121.46	0.34	C2-C3-C4	119.78	0.36
C3-C4-C4a	121.01	0.35	C6-C5-C4a	121.93	0.33	C5-C6-C6a	120.14	0.31
C13-C7-C6a	123.07	0.29	C13-C7-C7a	122.91	0.29	C6a-C7-C7a	114.00	0.26
C9-C8-C7a	119.36	0.33	C8-C9-C10	120.84	0.36	C9-C10-C11	120.12	0.37
C10-C11-C11a	119.68	0.33	C16-C12-C11a	121.74	0.28	C16-C12-C12a	124.85	0.28
C11a-C12-C12a	113.18	0.25	C7-C13-C14	122.27	0.31	C7-C13-C15	122.92	0.32
C14-C13-C15	114.74	0.31	N1-C14-C13	178.50	0.40	N2-C15-C13	177.49	0.45
C12-C16-C17	123.71	0.30	C12-C16-C18	123.12	0.31	C17-C16-C18	113.04	0.30
N3-C17-C16	175.90	0.39	N4-C18-C16	175.52	0.44	C1-C1a-C4a	118.00	0.28
C1-C1a-C12a	123.93	0.30	C4a-C1a-C12a	117.96	0.28	C4-C4a-C5	121.32	0.32
C4-C4a-C1a	119.39	0.31	C5-C4a-C1a	119.24	0.30	C6-C6a-C7	122.39	0.28
C6-C6a-C12a	119.89	0.28	C7-C6a-C12a	117.64	0.27	C7-C7a-C8	123.71	0.29
C7-C7a-C11a	116.38	0.27	C8-C7a-C11a	119.74	0.29	C11-C11a-C12	123.71	0.29
C11-C11a-C7a	120.22	0.29	C12-C11a-C7a	116.03	0.27	C12-C12a-C1a	124.00	0.27
C12-C12a-C6a	115.15	0.26	C1a-C12a-C6a	120.72	0.27			

Table 10. Dihedral Angles for **2j** and **3c**

Plane A	C8, C9, C10, C11, C11a, C7a
Plane B	C1, C2, C3, C4, C4a, C5, C6, C6a, C12a, C1a
Plane C	C6a, C7a, C11a, C12a
Plane D	C6a, C7, C7a, C13
Plane E	C7, C13, C14, C15, N1, N2
Plane F	C11a, C12a, C12, C16
Plane G	C12, C16, C17, C18, N3, N4

		Angle between the planes I and II/degree	
I	II	**2j**	**3c**
A	B	33.3(1)	49.5(1)
A	C	15.1(1)	25.2(1)
B	C	18.3(1)	24.4(1)
C	D	33.1(2)	34.4(2)
C	E		36.7(2)
C	F		41.0(2)
C	G		44.6(1)

pellets. Elemental analyses were performed at the Micro Analytical Center of Kyoto University. Cyclic voltammetry was performed with a PAR Model 174. The working electrode was platinum wire. A Ag/Ag^+ (0.1 M; 1 M=1 mol dm^{-3}) electrode was used as a reference and 0.1 M tetraethylammonium perchlorate as supporting electrolyte. The reduction potential was measured in a nitrogen-purged acetonitrile solution and the value measured was corrected to that relative to SCE (+0.24 V). The impedance measurements (pellet) were made in the frequency range 10 Hz—1 MHz using a gain-phase meter YHP 4276A LCZ METER at room temperature. All the solvents were used after distillation.

Starting Material. Quinone **1c** was purchased from Aldrich, Inc. and used without further purification. Quinones **1a—b, d—g** were prepared from naphthoquinone and the corresponding styrenes.[19] Quinone **4** was prepared according to the reported method.[20] Quinones **1h—l** were prepared by photochemical reactions of 2,3-dichloro-1,4-naphthoquinone with corresponding 1,1-diphenylethylenes.[21] Anthraquinone was purchased from Nacalai tesque Co. and used after recrystallization. TCNQ was prepared according to the reported method.[22]

Preparation of 2 and 3 (or 6). **2** and **3** (or **6**) were prepared according to Ong and Aumüller method. To a well-stirred mixture of 1 mmol of quinone **1** (or **4**) and 10 mmol of malononitrile in 20 ml of dichloromethane at an ice-bath temperature were added dropwise 10 ml of 1 mol dm^{-3} $TiCl_4$ solution and 20 mmol of pyridine. After end of addition, ice bath was removed to continue reaction at room temperature for overnight. The reaction mixture was treated with 50 ml of 10% aqueous HCl solution with vigorous stirring. Organic layer was separated and washed with brine and

dried. Purification of the products was accomplished by column chromatography developing hexane–benzene (2:1) and subsequently benzene. First bands contains **1** (or **6**), second one contains **2**, and third one contains **3**. The products were assigned from the following spectroscopic data.

7-Dicyanomethylene-2-fluoro-5-(4-fluorophenyl)benz[*a*]anthracen-12(7*H*)-one (2h): Red crystals from hexane–chloroform; mp>300 °C. MS; *m/z* 418 (M^+). Found: C, 77.57; H, 2.74; F, 8.91; N, 6.47%. Calcd for $C_{27}H_{12}F_2N_2O$: C, 77.51; H, 2.89; F, 9.08; N, 6.70%. IR (KBr); 2230 (C≡N), 1660 (C=O) cm^{-1}. ^1H NMR ($CDCl_3$) δ=7.2—8.5 (11H, m), 9.56 (1H, dd, *J*=11, 3 Hz). UV (CH_2Cl_2) λ_{max}: 234 (log ε=4.36), 257 (4.25), 315 (4.48), 377 (3.92), 422 (3.41) nm.

2-Chloro-5-(4-chlorophenyl)-7-(dicyanomethylene)benz[*a*]anthracen-12(7*H*)-one (2i): Orange crystals from hexane–chloroform; mp>300 °C. MS; *m/z* 450, 452, 454 (M^+). Found: C, 71.89; H, 2.61; Cl, 15.62; N, 6.17%. Calcd for $C_{27}H_{12}Cl_2N_2O$: C, 71.86; H, 2.68; Cl, 15.71; N, 6.21%. IR (KBr); 2210 (C≡N), 1650 (C=O) cm^{-1}. ^1H NMR ($CDCl_3$) δ=7.4—8.7 (11H, m), 9.88 (1H, d, *J*=3 Hz). UV (CH_2Cl_2) λ_{max}: 236 (4.56), 259 (4.38), 316 (4.56), 379 (4.01), 425 (3.50) nm.

7-Dicyanomethylene-5-phenylbenz[*a*]anthracen-12(7*H*)-one (2j): Orange crystals from hexane–chloroform; mp> 300 °C. MS; *m/z* 382 (M^+). Found: C, 85.08; H, 3.50; N, 7.31%. Calcd for $C_{27}H_{14}N_2O$: C, 84.80; H, 3.69; N, 7.33%. IR (KBr); 2200 (C≡N), 1650 (C=O) cm^{-1}. ^1H NMR ($CDCl_3$) δ=7.4—8.7 (13H, m), 9.77 (1H, d, *J*=10 Hz). UV (CH_2Cl_2) λ_{max}: 234 (4.46), 257 (4.27), 317 (4.61), 380 (3.98), 427 (3.49) nm.

7-Dicyanomethylene-2-methyl-5-(4-methylphenyl)benz[*a*]anthracen-12(7*H*)-one (2k): Orange needles from hexane–chloroform; mp>300 °C. MS; *m/z* 410 (M^+). Found: C, 84.85; H, 4.26; N, 7.00%. Calcd for $C_{29}H_{18}N_2O$: C, 84.86; H, 4.42; N, 6.82%. IR (KBr); 2230 (C≡N), 1650 (C=O) cm^{-1}. ^1H NMR ($CDCl_3$) δ=2.50 (3H, s), 2.68 (3H, s), 7.3—8.6 (11H, m), 9.58 (1H, s). UV (CH_2Cl_2) λ_{max}: 235 (4.51), 265 (4.33), 325 (4.58), 383 (3.96), 450 (3.46) nm.

7-Dicyanomethylene-2-methoxy-5-(4-methoxyphenyl)-benz[*a*]anthracen-12(7*H*)-one (2l): Red crystals from hexane–chloroform; mp>300 °C. MS; *m/z* 442 (M^+). Found: C, 78.79; H, 4.18; N, 6.14%. Calcd for $C_{29}H_{18}N_2O_3$: C, 78.72; H, 4.10; N, 6.33%. IR (KBr); 2220 (C≡N), 1640 (C=O) cm^{-1}. ^1H NMR ($CDCl_3$) δ=3.94 (3H, s), 4.12 (3H, s), 7.1—8.5 (11H, m), 9.32 (1H, d, *J*=3 Hz). UV (CH_2Cl_2) λ_{max}: 235 (4.63), 265 (4.45), 332 (4.58), 395 (3.97), 477 (3.61) nm.

7,12-Bis(dicyanomethylene)-2-fluoro-7,12-dihydrobenz[*a*]anthracene (3a): Orange cubics from acetonitrile; mp> 300 °C. MS; *m/z* 372 (M^+). Found: C, 77.51; H, 2.17; F, 5.16; N, 15.15%. Calcd for $C_{24}H_9FN_4$: C, 77.42; H, 2.44; F, 5.10; N, 15.05%. IR (KBr); 2240 (C≡N) cm^{-1}. ^1H NMR ($CDCl_3$) δ=7.54 (1H, m), 7.7—7.8 (3H, m), 8.04 (1H, m), 8.1—8.3 (4H, m). UV (CH_2Cl_2) λ_{max}: 232 (4.30), 285 (4.23), 334 (4.40), 424 (3.42) nm.

2-Chloro-7,12-bis(dicyanomethylene)-7,12-dihydrobenz[*a*]anthracene (3b): Orange cubics from acetonitrile; mp> 300 °C. High-resolution mass spectrum. Found: *m/z* 388.0521. Calcd for $C_{24}H_9N_4{}^{35}Cl$: M, 388.0515. Found: *m/z* 390.0483. Calcd for $C_{24}H_9N_4{}^{37}Cl$: M, 390.0486. IR (KBr); 2240 (C≡N) cm^{-1}. ^1H NMR ($CDCl_3$) δ=7.6—7.8 (3H, m), 7.97 (1H, d, *J*=8.9 Hz), 8.07 (1H, s), 8.17 (1H, d, *J*=8.5 Hz), 8.2—8.3 (3H, m). UV (CH_2Cl_2) λ_{max}: 232 (4.66), 286 (4.37), 336 (4.54), 426 (3.52) nm.

7,12-Bis(dicyanomethylene)-7,12-dihydrobenz[*a*]anthracene (3c): Orange plates from acetonitrile; mp>300 °C. MS; *m/z* 354 (M^+). Found: C, 81.29; H, 2.61; N, 15.76%. Calcd for $C_{24}H_{10}N_4$: C, 81.35; H, 2.84; N, 15.81%. IR (KBr); 2240 (C≡N) cm^{-1}. ^1H NMR ($CDCl_3$) δ=7.7—7.9 (4H, m), 8.02 (1H, d, *J*=8.2 Hz), 8.11 (1H, d, *J*=8.1 Hz), 8.1—8.3 (4H, m). UV (CH_2Cl_2) λ_{max}: 231 (4.29), 285 (4.19), 337 (4.46), 431 (3.46) nm.

7,12-Bis(dicyanomethylene)-2-methyl-7,12-dihydrobenz[*a*]-anthracene (3d): Red cubics from acetonitrile; mp>300 °C. MS; *m/z* 368 (M^+). Found: C, 81.32; H, 3.04; N, 15.51%. Calcd for $C_{24}H_{12}N_4$: C, 81.51; H, 3.28; N, 15.21%. IR (KBr); 2230 (C≡N) cm^{-1}. ^1H NMR ($CDCl_3$) δ=2.67 (3H, s), 7.57 (1H, d, *J*=8.2 Hz), 7.6—7.8 (2H, m), 7.83 (1H, s), 7.90 (1H, d, *J*=8.3 Hz), 8.12 (1H, d, *J*=8.2 Hz), 8.19 (1H, d, *J*=8.5 Hz), 8.2—8.3 (2H, m). UV (CH_2Cl_2) λ_{max}: 232 (4.42), 286 (4.28), 345 (4.48), 444 (3.43) nm.

7,12-Bis(dicyanomethylene)-2-methoxy-7,12-dihydrobenz[*a*]-anthracene (3e): Red crystals from acetonitrile; mp>300 °C. High-resolution mass spectrum. Found: *m/z* 384.1008. Calcd for $C_{25}H_{12}N_4O$: M, 384.1010. IR (KBr); 2230 (C≡N) cm^{-1}. ^1H NMR ($CDCl_3$) δ=4.08 (3H, s), 7.23 (1H, d, *J*=2.1 Hz), 7.39 (1H, dd, *J*=8.8, 2.1 Hz), 7.7—7.8 (2H, m), 7.90 (1H, d, *J*=9.2 Hz), 8.0—8.2 (2H, m), 8.2—8.3 (2H, m). UV (CH_2Cl_2) λ_{max}: 234 (4.56), 289 (4.39), 349 (4.39), 474 (3.41) nm.

7,12-Bis(dicyanomethylene)-3-methoxy-7,12-dihydrobenz-[*a*]anthracene (3f): Orange needles from acetonitrile; mp> 300 °C. MS; *m/z* 384 (M^+). Found: C, 78.27; H, 2.94; N, 14.42%. Calcd for $C_{25}H_{12}N_4O$: C, 78.12; H, 3.15; N, 14.58%. IR (KBr); 2230 (C≡N) cm^{-1}. ^1H NMR ($CDCl_3$) δ=3.99 (3H, s), 7.25 (1H, m), 7.44 (1H, dd, *J*=9.4, 2.4 Hz), 7.7—7.8 (2H, m), 7.98 (1H, d, *J*=9.4 Hz), 8.02 (1H, d, *J*=8.5 Hz), 8.1—8.3 (3H, m). UV (CH_2Cl_2) λ_{max}: 234 (4.54), 294 (4.28), 349 (4.56), 462 (3.76) nm.

7,12-Bis(dicyanomethylene)-4-methoxy-7,12-dihydrobenz-[*a*]anthracene (3g): Orange needles from acetonitrile; mp> 300 °C. MS; *m/z* 384 (M^+). Found: C, 78.40; H, 2.92; N, 14.51%. Calcd for $C_{25}H_{12}N_4O$: C, 78.12; H, 3.15; N, 14.58%. IR (KBr); 2230 (C≡N) cm^{-1}. ^1H NMR ($CDCl_3$) δ=4.06 (3H, s), 7.04 (1H, d, *J*=7.6 Hz), 7.63 (1H, d, *J*=8.8 Hz), 7.7—7.8 (3H, m), 8.2—8.3 (3H, m), 8.66 (1H, d, *J*=9.2 Hz). UV (CH_2Cl_2) λ_{max}: 233 (4.40), 286 (4.34), 346 (4.46), 480 (3.31) nm.

7,12-Bis(dicyanomethylene)-2-fluoro-5-(4-fluorophenyl)-7,12-dihydrobenz[*a*]anthracene (3h): Orange crystals from hexane–chloroform; mp>300 °C. High-resolution mass spectrum. Found: *m/z* 466.1029. Cacld for $C_{30}H_{12}F_2N_4$: M, 466.1029. IR (KBr); 2240 (C≡N) cm^{-1}. ^1H NMR ($CDCl_3$) δ=7.3—8.6 (12H, m). UV (CH_2Cl_2) λ_{max}: 234 (4.51), 287 (4.35), 343 (4.49), 449 (3.64) nm.

2-Chloro-5-(4-chlorophenyl)-7,12-bis(dicyanomethylene)-7,12-dihydrobenz[*a*]anthracene (3i): Orange crystals from hexane–chloroform; mp>300 °C. MS; *m/z* 498, 500, 502 (M^+). Found: C, 71.96; H, 2.30; Cl, 14.43; N, 11.14%. Calcd for $C_{30}H_{12}Cl_2N_4$: C, 72.16; H, 2.42; Cl, 14.20; N, 11.22%. IR (KBr); 2250 (C≡N) cm^{-1}. ^1H NMR ($CDCl_3$) δ=7.4—8.7 (12H, m). UV (CH_2Cl_2) λ_{max}: 234 (4.59), 288 (4.33), 343 (4.48), 458 (3.59) nm.

7,12-Bis(dicyanomethylene)-5-phenyl-7,12-dihydrobenz[*a*]-anthracene (3j): Red crystals from hexane–chloroform; mp>300 °C. MS; *m/z* 430 (M^+). Found: C, 83.67; H, 3.15; N,

12.79%. Calcd for $C_{30}H_{14}N_4$: C, 83.71; H, 3.28; N, 13.02%. IR (KBr); 2240 (C≡N) cm^{-1}. ^1H NMR ($CDCl_3$) δ=7.6—8.7 (14H, m). UV (CH_2Cl_2) λ_{max}: 233 (4.56), 288 (4.40), 345 (4.61), 458 (3.70) nm.

7,12-Bis(dicyanomethylene)-2-methyl-5-(4-methylphenyl)-7,12-dihydrobenz[a]anthracene (3k): Orange crystals from hexane–chloroform; mp>300 °C. MS; *m/z* 458 (M^+). Found: C, 84.02; H, 3.83; N, 11.96%. Calcd for $C_{32}H_{18}N_4$: C, 83.82; H, 3.96; N, 12.22%. IR (KBr); 2230 (C≡N) cm^{-1}. ^1H NMR ($CDCl_3$) δ=2.50 (3H, s), 2.71 (3H, s), 7.2—8.8 (12H, m). UV (CH_2Cl_2) λ_{max}: 236 (4.60), 290 (4.47), 354 (4.59), 478 (3.70) nm.

7,12-Bis(dicyanomethylene)-2-methoxy-5-(4-methoxyphenyl)-7,12-dihydrobenz[a]anthracene (3l): Purple crystals from hexane–chloroform; mp>300 °C. MS; *m/z* 490 (M^+). Found: C, 78.09; H, 3.43; N, 11.42%. Calcd for $C_{32}H_{18}N_4O_2$: C, 78.36; H, 3.70; N, 11.42%. IR (KBr); 2220 (C≡N) cm^{-1}. ^1H NMR ($CDCl_3$) δ=3.92 (3H, s), 4.11 (3H, s), 7.0—8.5 (12H, m). UV (CH_2Cl_2) λ_{max}: 238 (4.61), 287 (4.45), 358 (4.45), 502 (3.68) nm.

5,12-Bis(dicyanomethylene)-5,12-dihydronaphthacene (6): Yellow needles from hexane–chloroform; mp>300 °C. MS; *m/z* 354 (M^+). Found: C, 81.10; H, 2.66; N, 15.64%. Calcd for $C_{25}H_{12}N_4$: C, 81.35; H, 2.84; N, 15.81%. IR (KBr); 2240 (C≡N) cm^{-1}. ^1H NMR ($CDCl_3$) δ=7.76 (4H, m), 8.05 (2H, m), 8.27 (2H, m), 8.72 (2H, s). UV (CH_2Cl_2) λ_{max}: 233 (4.39), 260 (4.51), 306 (4.51), 424 (3.96) nm.

Molecular Complexes of 3c. Naphthalene, pyrene, anthracene was purchased from Nacalai tesque Co. and used after recrystallization. TMTTF was prepared according to the reported method.[23] **3c** and an excess amounts of a donor were dissolved in dichloromethane, and ethanol was added to precipitate a complex and prevent the precipitate of excess donor. The mixture was concentrated by distillation, and then cooled, but complex did not precipitate. However, a dichloromethane solution containing **3c** (0.0025 mol dm^{-3}) and donors (0.05 mol dm^{-3}) showed a CT band, which was obtained by substracting the "background" absorption of samples (absorption of **3c** and donors). Intensity of these CT bands increased as donors were added into the mixture.

X-Ray Structure Analyses. The X-ray structure analyses were made with a Rigaku Denki AFC-4 automatic four-circle diffractometer [Ni-filtered Cu $K\alpha$ radiation (154.184 pm), ω–2θ scan technique, $2\theta \leqq 120°$, scan speed 4° min^{-1} (θ), scan range (1.5+0.15 tan θ)°]. Three standard reflections measured every 100 reflections showed no significant X-ray damage or crystal decay. Unique 3031 (for **2j**) and 2792 (for **3c**) reflections were used for structure determination. The structure was solved by direct methods with MULTAN 78[24] (with atomic scattering factors from International Tables for X-ray Crystallography)[25] and refined by block-diagonal least squares[26] with anisotropic thermal parameters for non-hydrogen atoms and isotropic for hydrogen atoms. **2j**: R=0.0754 and R_2=0.0681, where ω=1.0 for Fobs≠0, ω=0.8 for Fobs=0.0, **3c**: R=0.0589 and R_2=0.0656 where ω=1.0 for Fobs≠0, ω=0.8 for Fobs=0.0. Crystal data are as follows; **2j**: a=1150.0 (1), b=1163.0 (1), c=815.4 (1) pm, α=106.31 (1), β=89.33 (1), γ=116.29 (1)°, space group=P-1 (triclinic) (Z=2). V=9.303×10^8 (1) pm^3, D_c/g cm^{-3}=1.366 (1). **3c**: a=891.4 (1), b=1489.0 (1), c=733.8 (1) pm, α=90.67 (1), β=110.36 (1), γ=104.00 (1)°, space group=P-1 (triclinic) (Z=2). V=8.812×10^8 (1) pm^3, D_c/g cm^{-3}=1.336 (1).

We are grateful to Professor Yukiteru Katsube and his co-worker at Institute for Protein Research, Osaka University, for the measurement of X-ray analyses.

References

1) A. F. Garito and A. J. Heeger, *Acc. Chem. Res.*, **7**, 232 (1974). J. H. Perlstein, *Angew. Chem., Int. Ed. Engl.*, **16**, 519 (1977). J. B. Torrance, *Acc. Chem. Res.*, **12**, 79 (1979). F. Wudl, "The Physics and Chemistry of Low Dimensional Solids," ed by L. Alcácer and D. Reidel, Dordrecht, Holland (1980). D. O. Cowan, A. Kini, L-Y. Chiang, K. Lerstrup, D. R. Talham, T. O. Poehler, and A. N. Bloch, *Mol. Cryst. Liq. Cryst.*, **86**, 1 (1982). "Dendōusei Teizigen Busshitsu no Kagaku," Kagaku Sosetsu, No. 42, Gakkai Shuppan Center, Tokyo (1983). F. Wudl, *Acc. Chem. Res.*, **17**, 227 (1984). J. M. Williams, M. A. Beno, H. H. Wang, P. C. W. Leung, T. J. Emge, U. Geiser, and K. D. Carlson, *Acc. Chem. Res.*, **18**, 261 (1985), and references therein.

2) U. Schubert, S. Hünig, and A. Aumüller, *Liebigs Ann. Chem.*, **1985**, 1216. C. Kabuto, Y. Fukazawa, T. Suzuki, Y. Yamashita, T. Miyashi, and T. Mukai, *Tetrahedron Lett.*, **27**, 925 (1986).

3) T. Mukai, T. Suzuki, and Y. Yamashita, *Bull. Chem. Soc. Jpn.*, **58**, 2433 (1985). Y. Nishizawa, T. Suzuki, Y. Yamashita, T. Miyashi, and T. Mukai, *Nippon Kagaku Kaishi*, **1985**, 904.

4) A. Aumüller and S. Hünig, *Ann. Chem.*, **1984**, 618.

5) B. S. Ong and B. Keoshkerian, *J. Org. Chem.*, **49**, 5002 (1984).

6) Y. Yamashita, T. Suzuki, and T. Mukai, *Nippon Kagaku Kaishi*, **1986**, 268.

7) A. M. Kini, D. O. Cowan, F. Gerson, and R. Möckel, *J. Am. Chem. Soc.*, **107**, 556 (1985).

8) Since the UV measurements were carried out in 10^{-4}—10^{-5} mol dm^{-3}, the possibility of intermolecular CT interaction could be eliminated.

9) E. M. Kosower, "An Introduction to Physical Organic Chemistry," Wiley, New York (1968).

10) R. L. Myers and I. Shain, *Anal. Chem.*, **41**, 980 (1969).

11) F. Gerson, R. Heckendorn, D. O. Cowan, A. M. Kini, and M. Maxfield, *J. Am. Chem. Soc.*, **105**, 7017 (1983).

12) We attempted to observe radical anion and radical trianion of **3c** by ESR method, but none of the spectra could be unequivocally be attributed to them because of the complicated ESR signals.

13) B. Rosenau, C. Krieger, and H. A. Staab, *Tetrahedron Lett.*, **26**, 2081 (1985).

14) A. Kini, M. Mays, and D. O. Cowan, *J. Chem. Soc., Chem. Commun.*, **1985**, 286.

15) J. Silverman and N. F. Yannoni, *J. Chem. Soc. B*, **1967**, 194.

16) R. P. Ferrier and J. Iball, *Acta Crystallogr.*, **16**, 269 (1963).

17) F. Iwasaki, *Acta Crystallogr., Sect. B*, **27**, 1360 (1971).

18) S. Yamaguchi, T. Hanafusa, T. Tanaka, M. Sawada, K. Kondo, M. Irie, H. Tatemitsu, Y. Sakata, and S. Misumi, *Tetrahedron Lett.*, **27**, 2411 (1986).

19) G. M. Muschik, J. E. Tomaszewski, R. I. Sato, and W. B. Manning, *J. Org. Chem.*, **44**, 2150 (1979).

20) M. P. Cava, A. A. Deana, and K. Muth, *J. Am. Chem. Soc.*, **81**, 6458 (1959).

21) K. Maruyama, T. Otsuki, and S. Tai, *J. Org. Chem.*, **50**, 52 (1985).
22) D. S. Acker and W. R. Hertler, *J. Am. Chem. Soc.*, **84**, 3370 (1962).
23) J. P. Ferraris, T. O. Poehler, A. N. Bloch, and D. O. Cowan, *Tetrahedron Lett.*, **27**, 2553 (1973).
24) P. Main, S. E. Hull, L. Lessinger, G. Germain, J. -P. Declercq, and M. M. Woolfson, "A System of Computer Programs for the Automatic Solution of Crystal Structures from X-ray Diffraction Data, MULTAN 78," University of York (England) and Louvain (Belgium) (1978).
25) "International Tables for X-ray Crystallography," Vol. 4, ed by J. A. Ibers and W. C. Hamilton, Birmingham, Kynoch Press (1974).
26) T. Ashida, HBLS 5 "The Universal Crystallographic Computing System Osaka," The Computation Center, Osaka University, 53 (1979).